High-performance liquid chromatography coupled to ultraviolet diode array detection and electrospray ionization mass spectrometry for the analysis of intermediates produced in the initial steps of the photocatalytic degradation of sulfonated azo dyes

Alessandra Bianco Prevot[*], Debora Fabbri, Edmondo Pramauro, Claudio Baiocchi, Claudio Medana

Dipartimento di Chimica Analitica, Via Pietro Giuria 5, 10125 Torino, Italy

ABSTRACT

High-performance liquid chromatography coupled to ultraviolet diode array detection and electrospray ionization mass spectrometry was applied to monitor the photocatalytic degradation mediated by TiO$_2$ of three sulfonated monoazo dyes (Orange I, Orange II, and Ethylorange) present in aqueous solution. Photo-bleaching, organic carbon, nitrogen and sulfur evolution were also followed during the process. Delayed carbon mineralization was observed with respect to both dyes disappearance and photobleaching, due to the formation of transient intermediate compounds which were in turn completely degraded. Among the intermediates produced during the initial degradation steps the formation of several hydroxylated derivatives, mostly coloured, was evidenced. The MS^2 spectra allowed one to formulate hypothesis about the OH attack positions; a peculiar reactivity of the azo moiety was shown by Orange I and Orange II.

© 2008 Elsevier B.V. All rights reserved.

1. Introduction

In textile industry more than 100,000 different dyes are commercially available and it is estimated that about 15% of the world dyes production is lost during the dyeing process [1,2].

Azo dyes represent more than 50% of the total dyes amount and if present in the effluents of textile industry they are not only undesirable because of their colour but also because they can undergo reduction producing carcinogenic aromatic amines [3,4]; for these reasons an efficient degradation process is needed for the treatment of either industrial wastes or polluted natural water streams. Azo dyes are recalcitrant to aerobic degradation in municipal sewerage systems [5] and the common water treatments (precipitation, flocculation, adsorption on active carbon) only displace the problem and require further sludge treatment or carbon regeneration [6]. An alternative is represented by the Advanced Oxidation Processes (AOP's), able to degrade organic compounds until their mineralization occurs; among them heterogeneous photocatalysis in the presence of TiO$_2$ suspensions has been shown to be convenient

since it operates at ambient condition and it uses a cheap and safe catalyst, atmospheric oxygen and solar light (or simulated) [7,8]. Many papers have been published concerning the TiO$_2$ mediated degradation of azo dyes in aqueous solutions and recently an exhaustive review appeared about this topic [9–13]. Most of these papers deal with the process parameters optimization and give an overlook of the process efficiency by monitoring the DOC evolution. Only few of them investigate the nature of the intermediates formed during the degradation and even in these cases the discussion concerns the nature of compounds formed after the chromophore cleavage and the molecule rupture, with particular attention to establish whether the attack occurs directly on the azo-group or on the C atom bearing it. GC–MS and FTIR have been reported in the literature as suitable methods for the assessment of the identity of Orange II intermediates, either in solution (after extraction with organic solvent) or starting from the dye adsorbed on the semiconductor [14,15]; recently ESI-MS technique has been proposed for the monitoring of the degradation of azo dyes [16]. At our knowledge there is generally a lack of information about the nature of intermediates formed during the initial degradation steps, in particular those still retaining the chromophoric group [17]. In the present research the degradation of three commercial sulfonated azo dyes (Fig. 1) has been attempted,

* Corresponding author. Tel.: +39 0116707634; fax: +39 0116707615.
E-mail address: alessandra.biancoprevot@unito.it (A. Bianco Prevot).
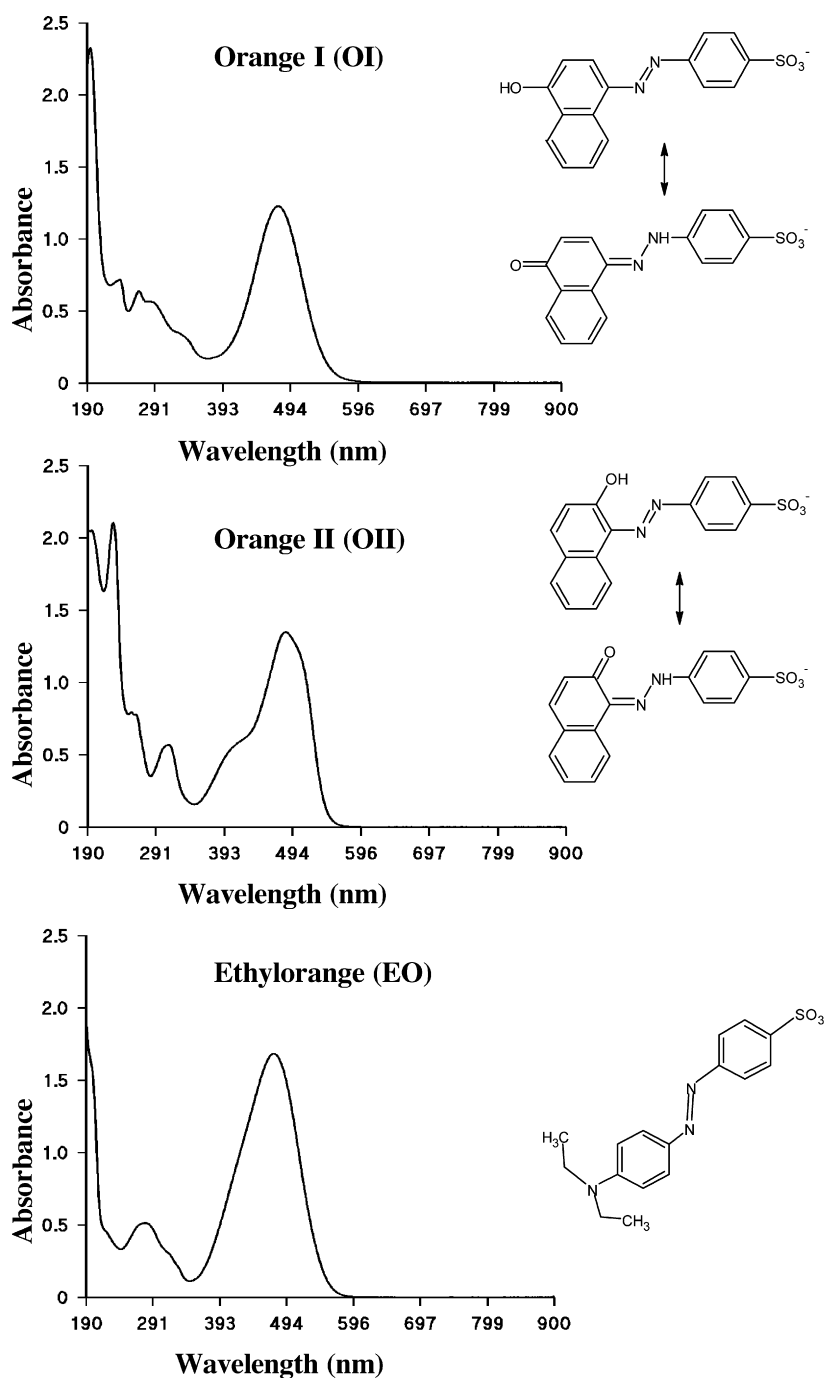
Fig. 1. Structure and UV–vis spectrum of the investigated dyes.

with particular attention devoted to the identification of the initial coloured and/or sulfonated intermediates. Beside their importance under the mechanicistic point of view, eventually formed coloured intermediates are also of environmental concern and sulfonated derivatives, being highly soluble in water and mobile in this environmental compartment, can extend the potential pollution risk. Among the chosen dyes, many authors have considered Orange II as an azo dye model and thus its TiO$_2$ mediated photodegradation was the object of studies concerning its degradability and other related topics [18–22].

Since sulfonated azo dyes have in general poor thermal stability and low volatility we considered the high-performance liquid chromatography coupled to ultraviolet diode array detection and electrospray ionization mass spectrometry (HPLC–DAD-ESI–MS) a suitable analytical approach for their determination together with their hydrophilic initial degradation products, without the needing of any derivatization and/or solvent extraction steps.

2. Experimental

2.1. Reagents and materials

The following sulfonated azo dyes were provided by Aldrich and were used without further purification: Orange I (OI, M.W.

350.32, CAS no. 523–44–4, λ_{max} 476 nm), Orange II (OII, M.W. 350.32, CAS no. 633–96–5, λ_{max} 484 nm,), Ethylorange (EO, M.W. 355.39, CAS no. 62758–12–7, λ_{max} 474 nm). All the other indicated reagents were of analytical grade (Merck) and were used as received: ammonium acetate, acetonitrile (Lichrosolv), K_2CO_3, Na_2CO_3, $NaHCO_3$ (Merck). Ultra pure water was provided by a Milli-Q^{TM} system (Millipore). TiO_2 P25 from Degussa (ca. 80% anatase form) having a surface area of ca. $55\,m^2\,g^{-1}$ was used in all the photocatalytic experiments. The semiconductor was preliminarily irradiated overnight to eliminate adsorbed organics and successively washed repeatedly with water. After centrifugation, the solid material was dried in oven (ca. 12 h at 80 °C) and stored in a closed glass container. The resulting powder was resuspended in water by sonication immediately before use.

2.2. Degradation procedures

The degradation experiments were performed under aerobic conditions irradiating 500 mL of aqueous solutions containing $20\,mg\,L^{-1}$ of a single dye and $400\,mg\,L^{-1}$ of TiO_2 in a cylindrical photochemical reactor (Helios-Italquartz, Milan), equipped with a 125 W medium pressure Hg lamp. The system was kept under continuous stirring in order to avoid the formation of concentration gradient and to favour the oxygen supply. Cold water circulating in the jacket surrounding the lamp kept the temperature within the reactor at 20 °C; a Pyrex® glass jacket acting as a cut-off filter for wavelengths below 300 nm was employed, in order to avoid any possible contribution coming from dye photolysis.

All the analytical determinations were performed on 5.0 mL samples, taken from the reactor after defined irradiation times and successively filtered through a 0.45 μm Millex–HA membrane.

The analysis of the transient intermediates was performed on 15 mL samples, filtered and concentrated to ca. 1 mL by means of evaporation under vacuum at low temperature.

2.3. Analytical procedures

HPLC–DAD–ESI–MS[n] analysis were performed by means of Dionex Ultimate 3000 under gradient conditions using a Varian Pursuit XRs 3u C-18 column (250 mm × 2.0 mm) and a mobile phase composed of acetonitrile–ammonium acetate 0.1 mM (5/95, v/v to 100/0 in 30 min), at pH 6.8, flow rate 0.2 mL/min. The eluent from the chromatographic column successively enters the UV–vis diode array detector (Thermo Surveyor), the ESI interface and the Thermo LTQ ion trap mass spectrometer. MS and MS[n] analyses were performed in the negative ion mode; the mass range was 100–350 m/z. High purity nitrogen was used as nebulizer and auxiliary gas operating pressure at 20 and 5 units, respectively, of the 0–100 arbitrary scale of the instrument. The ESI probe tip and capillary potentials were set at −4.5 kV and −19 V, respectively. The heated capillary was set to 275 °C the tube lens voltage to −73.5 V.

The inorganic ions formed upon the mineralization of organic N and S were determined using an IC Dionex DX 500 equipped with a gradient pump GP-40 and electrochemical detector ED 40 (Dionex). A 200 mm long × 4 mm i.d. CS12A column was used for the determination of ammonium, with 25 mM metansulfonic acid at a flow rate of $1\,mL\,min^{-1}$ as eluent. Nitrate and sulfate have been analysed by using a 200 mm long × 4 mm i.d. AS9-HC column (Dionex). The eluent was a solution containing K_2CO_3 10 mM and $NaHCO_3$ 4 mM; elutions were performed at 30 °C, at a flow rate of $1.0\,mL\,min^{-1}$.

The dissolved organic carbon (DOC) was measured on filtered samples using a Shimadzu TOC-5000 analyser (catalytic oxidation on Pt at 680 °C) previously calibrated using standard solutions of potassium phthalate.

3. Results and discussion

3.1. Primary degradation and mineralization process

The TiO_2 mediated photodegradation process has been widely discussed in the literature; it is well established that when a TiO_2 aqueous suspension is irradiated with light having energy greater than the semiconductor band gap, electron and holes are formed in the conduction and in the valence band, respectively. These species
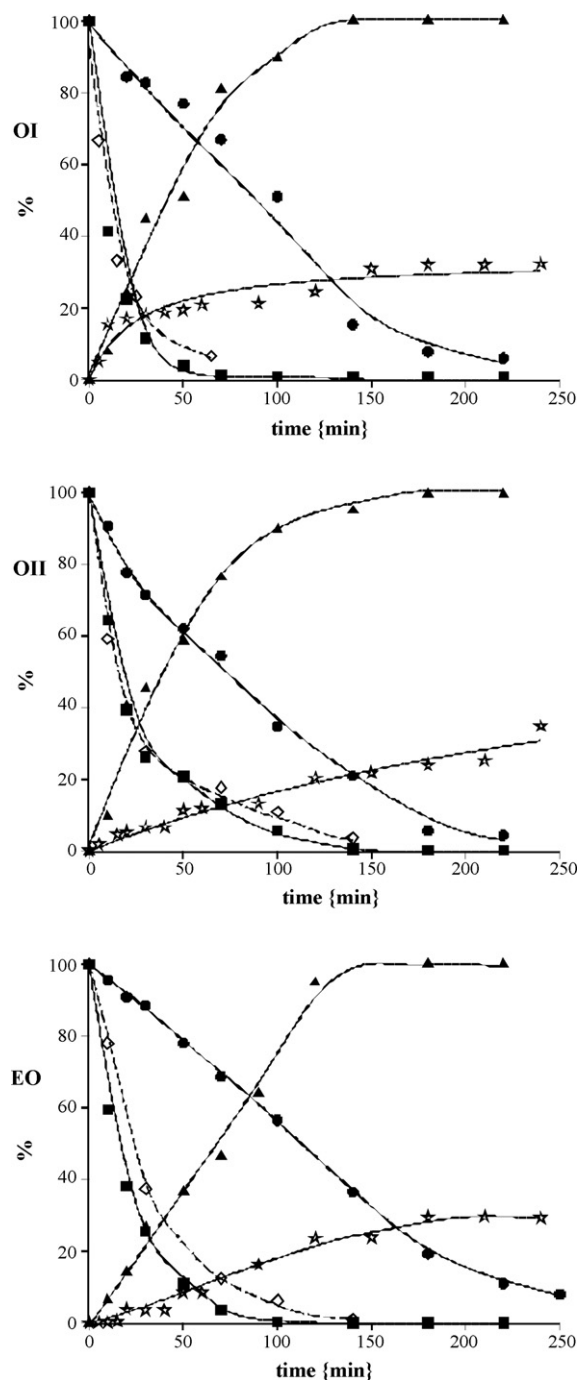
Fig. 2. Photocatalytic degradation of dyes. (■) Percentage of substrate abatement, (●) decrease percentage of DOC, (◇) decrease percentage of relative absorbance at wavelength of maximum adsorption, (▲) percentage of sulfate released in solution, (☆) sum of nitrogen mineralization species (nitrate, nitrite and ammonium) released in solution.

can migrate to the catalyst surface and react with oxygen (electrons) and with the trapped hydroxyl ions (holes); among the products of a series of reactions the hydroxyl radical is the strongest oxidant formed; it can in turn attack the organic substrates present in solution close to or adsorbed on the catalyst surface, finally yielding to the substrate mineralization. In addition to this process a direct reduction or oxidation between the substrate and the electrons or the holes, respectively, can take place.

In the presence of dissolved species able to absorb the visible light also the contribution of photosensitized oxidation can be invoked; the dyes excitation can in fact be followed by electron injection on the TiO_2 conduction band [23], with further OH radical formation and dyes degradation. Due to the similarity in the degradation mechanism it is not always possible to distinguish these two processes; the photosensitized oxidation allows one to operate the dyes treatment also in the presence of radiation with a low UV contribution (i.e. solar light) [15].

The typical emission spectrum of the lamp employed in this study allows the presence of both the processes. No evidence of photolysis appeared from irradiation experiments performed in the absence of TiO_2.

Fig. 2 shows the profiles of dyes disappearance, photobleaching (determined by following the absorbance decrease in the VIS absorption range of the dyes) and DOC and inorganic products evolution for the investigated substrates. When the dyes degradation is compared with the trend of absorbance in the visible region it

can be noticed that the photobleaching is delayed and this can be due to the formation of intermediates also contributing to the solution colour. In the case of OI and OII a slight difference between the two processes can be observed only in the last part of the dye degradation profile suggesting that the chromophore cleavage is the main degradation step. On the contrary, EO behaviour suggests the formation and accumulation of coloured intermediates.

When comparing the behaviour of OI and OII, a faster substrate degradation can be observed for OI, completely transformed in about half the time necessary for OII disappearance. Analogous results have been previously reported by Yang et al. [24]; they suggest that OII degradation can be regarded as partly hole-mediated process whereas a chiefly hole-mediated mechanism is proposed for OI. This hypothesis is consistent with the higher adsorption extent observed for OI on the TiO_2 surface. On the other hand OI and OII show a very similar DOC evolution profile, allowing one to suppose the formation of the same and/or less adsorbed intermediate products.

For all the examined dyes the accumulation of organic intermediates is consistent with the observed DOC abatement, since at the time corresponding to the complete dyes disappearance significant amounts of organic carbon are still present. They in turn degrade, yielding to the complete carbon mineralization.

As for sulfur fate is concerned, at the time corresponding to the complete dyes disappearance, the sulfate released in solution is
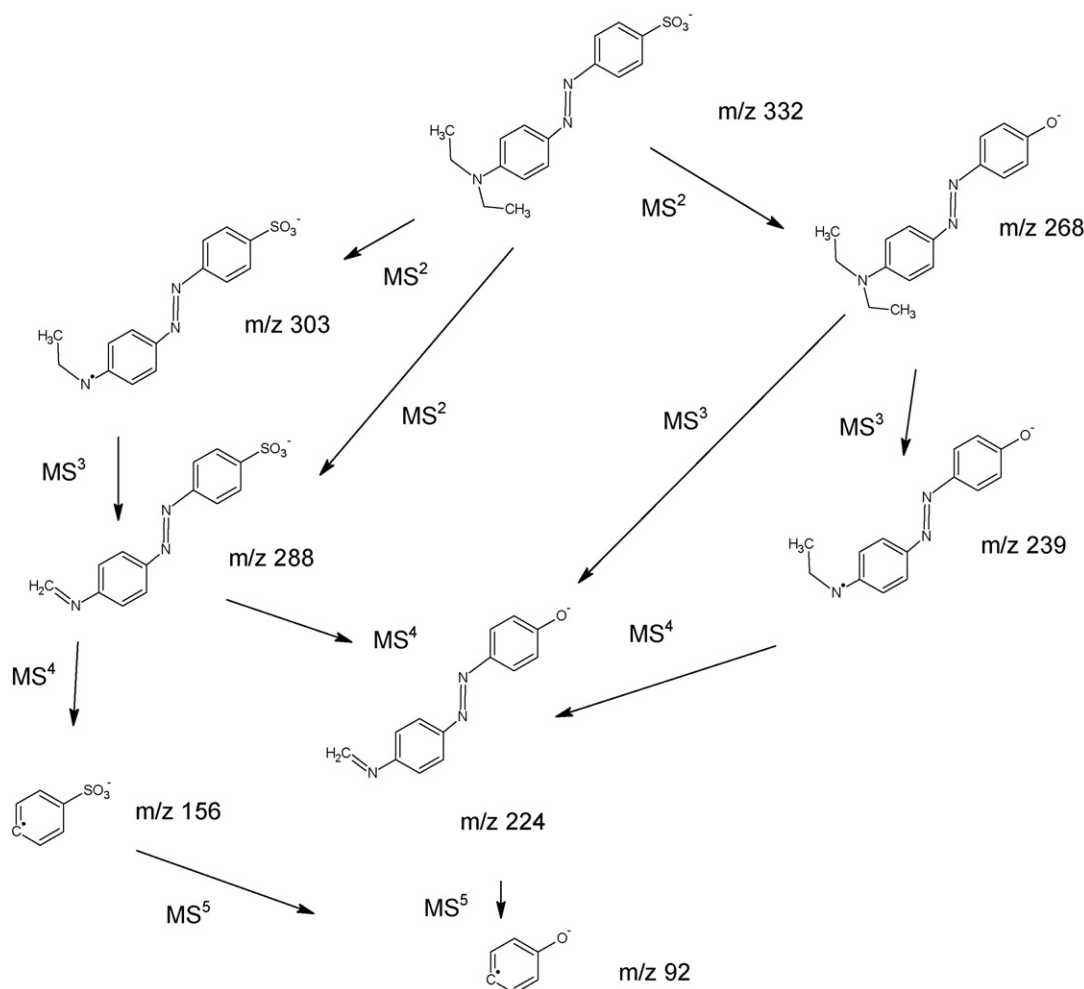

Fig. 3. MS^n fragmentation of Ethylorange.

below the stoichiometric amount (see Fig. 2); this value is reached, for all the examined dyes, at irradiation time corresponding to the complete DOC abatement; the delay observed between dyes abatement and sulfate evolution allows one to suppose the formation of sulfonated intermediates.

On the contrary, the sum of nitrate, nitrite and ammonium detected was lower than the nitrogen stoichiometric amount even at irradiation time corresponding to the complete organic carbon mineralization (see Fig. 2). A lack in the nitrogen mass balance has been already reported and the formation of molecular nitrogen has been proposed in the literature as a possible explanation [8,25].

3.2. Intermediates characterization

In agreement with the previous discussed DOC and photobleaching evidences, HPLC–DAD-ESI–MS analyses performed on irradiated samples show the presence of many intermediates (mainly coloured).
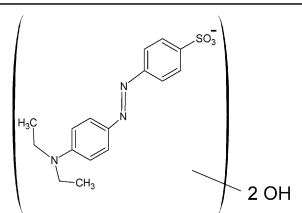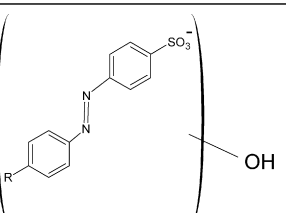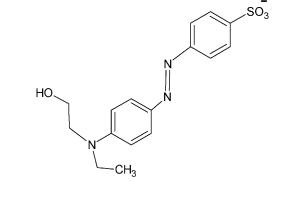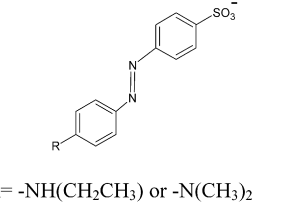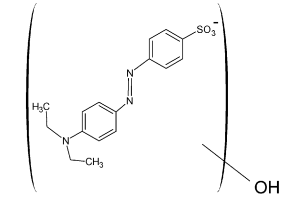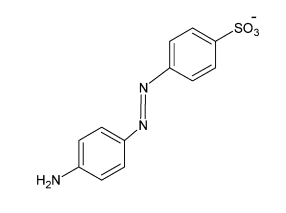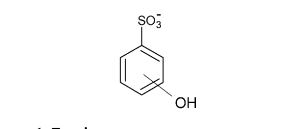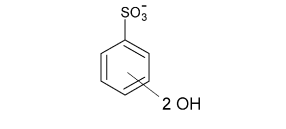
3.2.1. Ethylorange

The parent molecule of Ethylorange exhibits a precursor ion at m/z 332 as base peak and Fig. 3 reports the EO fragmentation proposed on the basis of MS^n (with n up to 5) spectrum. It is possible to observe the presence of odd electron species, coming from the homolytic breakdown; this peculiar event is scarcely present in electrospray ionization owing to the fact that only even electron ions $[M+H^-]$ or $[M-H^-]$ are formed. However, this occurrence was previously observed and explained in the case of Methylorange [11] and could thus justify the behaviour of the homologous Ethylorange. The great structural stability of Ethylorange molecule due to the extended electron conjugation makes possible more energetic and so less probable fragmentation pathway involving radical formation.

Among the proposed structures the fragments having m/z 156, 239, 288 and 303 appear to be discriminating in the intermediates identification, as discussed later on.

In Table 1 the structure of the intermediates formed after 15 min irradiation of an EO sample is reported together with the

Table 1
Ethylorange degradation: intermediates detected after 15 min irradiation

m/z	structure	m/z	structure
364	H₃C–N(–CH₃)–C₆H₄–N=N–C₆H₄–SO₃⁻ ( ) 2 OH t_R = 14.8 min 16.7 min 17.3 min	320	R–C₆H₄–N=N–C₆H₄–SO₃⁻ ( ) OH R= -NH(CH₂CH₃) or -N(CH₃)₂ t_R = 12.8 min 13.1 min 15.1 min 15.6 min
348	HO–CH₂CH₂–N(–CH₃)–C₆H₄–N=N–C₆H₄–SO₃⁻ t_R = 14.6 min	304	R–C₆H₄–N=N–C₆H₄–SO₃⁻ R= -NH(CH₂CH₃) or -N(CH₃)₂ t_R = 15.3 min
348	H₃C–N(–CH₂CH₃)(–CH₃)–C₆H₄–N=N–C₆H₄–SO₃⁻ ( ) OH t_R = 15.7 min 16.3 min 16.8 min 17.2 min	276	H₂N–C₆H₄–N=N–C₆H₄–SO₃⁻ t_R = 12.3 min
173	C₆H₄(OH)(SO₃⁻) t_R = 1.7 min	189	C₆H₃(OH)₂(SO₃⁻) 2 OH t_R = 1.6 min
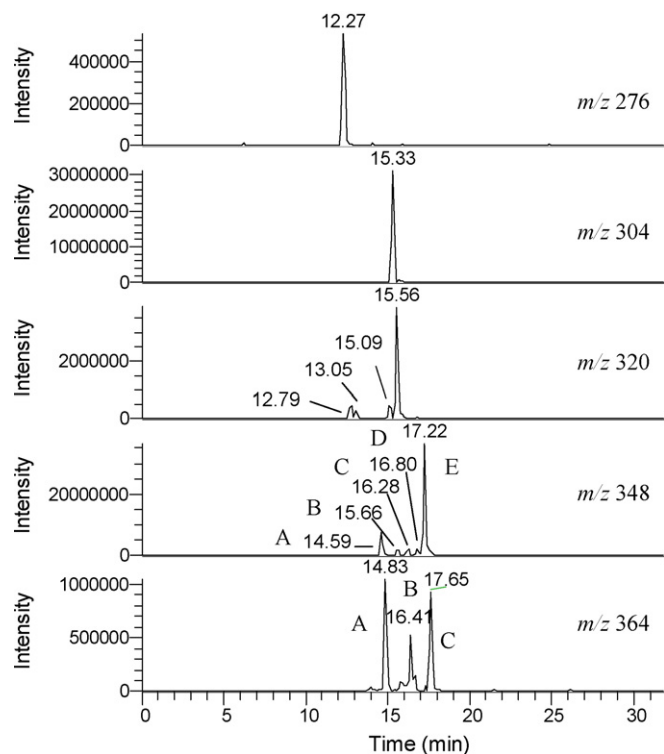
Fig. 4. LC–MS pattern of the EO sample at 15 min of degradation displayed at different m/z values.

Fig. 5. MS^2 spectrum and fragmentation of intermediates reported as A and E in the text, having m/z 348.

corresponding m/z value and retention times. Fig. 4 shows the digital reconstructions, at various significant m/z values, of the corresponding chromatogram. Five peaks have been found when extracting from the total ionic current the m/z 348; this value is higher than that of the parent molecule and consistent with the hypothesis of the formation of mono-hydroxylated products; in theory five different positions are available on the EO molecule for the OH radical attack, usually not selective. From the MS^2 spectra useful informations were obtained in order to identify the different possible isomers and Fig. 5 reports the fragmentation spectra of the structures proposed for the two most abundant peaks (A and E). For compound A (t_R = 14.6) the presence of the odd electron ions at m/z 156 is not compatible with the OH attack on the ring bearing the SO$_3$$^-$ group; moreover, fragments having m/z 239, 288 and 303 (already detected in the EO fragmentation) and m/z 260 can be explained only hypothesizing the introduction of one OH in the lateral chain. For compounds E (t_R = 17.2) the absence of the phenylsulfonic radical (m/z 156) and the presence of a fragment with m/z 172, corresponding to the hydroxyphenylsulfonic radical allows one to suppose the introduction of the OH group in the sulfonated ring. The withdrawing nature of the sulfonic group reduces the electronic density of the ring which becomes less reactive towards the electrophilic attack by •OH, but the meta position in respect to the sulfonic group is relatively less deactivated and hydroxylation in this position should probably occur. Nevertheless, recently published results [26] indicate that the primary photocatalytic oxidation of aromatic compounds containing an electron withdrawing group gives rise to the formation of all the monohydroxy derivatives. Moreover, the retention time of the compound E, not only the highest among the m/z 348 fragments but also slightly higher than the t_R of Ethylorange (t_R = 17.0), suggests an OH attack in *ortho* position with respect to –SO$_3$$^-$; the stabilizing effect of OH would make this molecule less hydrophilic, thus enhancing the interaction with the stationary phase. The MS spec-
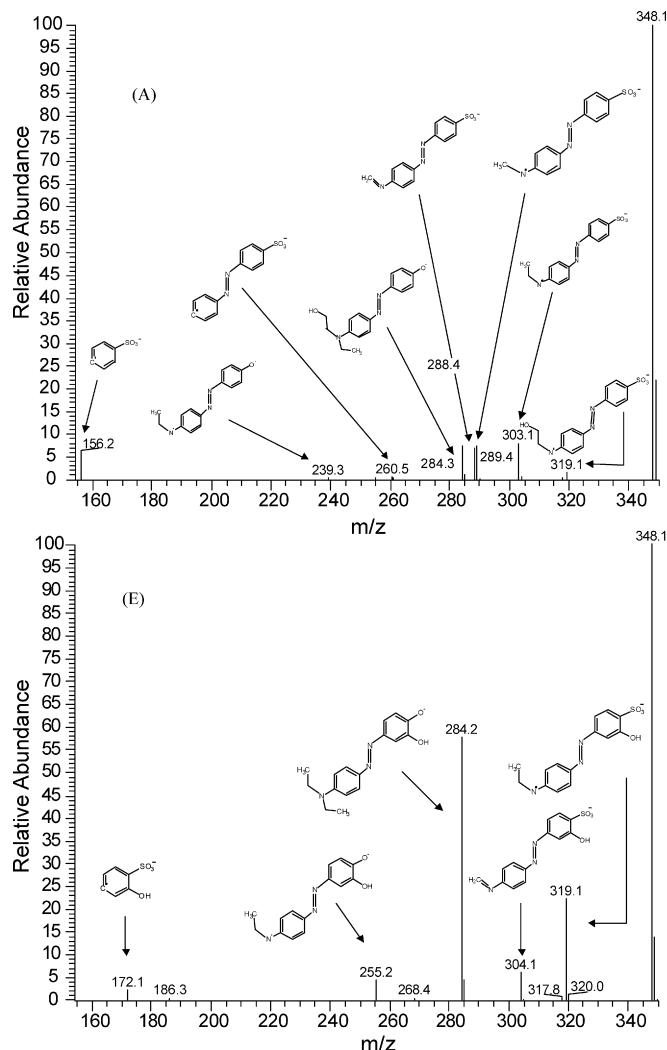
tra of the peaks corresponding to the other isomers, present at trace levels, do not bring enough information for the assessment of the OH position.

For what concerns the other intermediates, the presence of three peaks having m/z 364 can be explained by the formation of di-hydroxylated intermediates. Fig. 6 shows the MS^2 spectrum of the more abundant peak (t_R = 14.83 min); for sake of brevity the MS^2 spectra of the other peaks are not reported since they all show a very similar fragmentation path. The absence in the spectrum of the fragment with m/z 156 and the presence of the fragment with m/z 172 allows one to suppose the addition of one OH on the sulfonated ring; in analogy with the previously discussed structure of the mono-hydroxylated intermediates it is reasonable to suppose its position in *ortho* with respect to the sulfonic group for the compound having the highest t_R. Moreover the presence of a fragment with m/z 319, corresponding to a loss of the C$_2$H$_5$O radical points to the addition of the second OH on the alkyl chain.

Mono- and dihydroxhybenzensulfonates were also detected at the trace levels.

Parallel to a degradation mechanism leading to hydroxy derivatives, many intermediates coming out from the partial degradation of the alkyl moiety have been also identified (m/z 276, 304 and 320
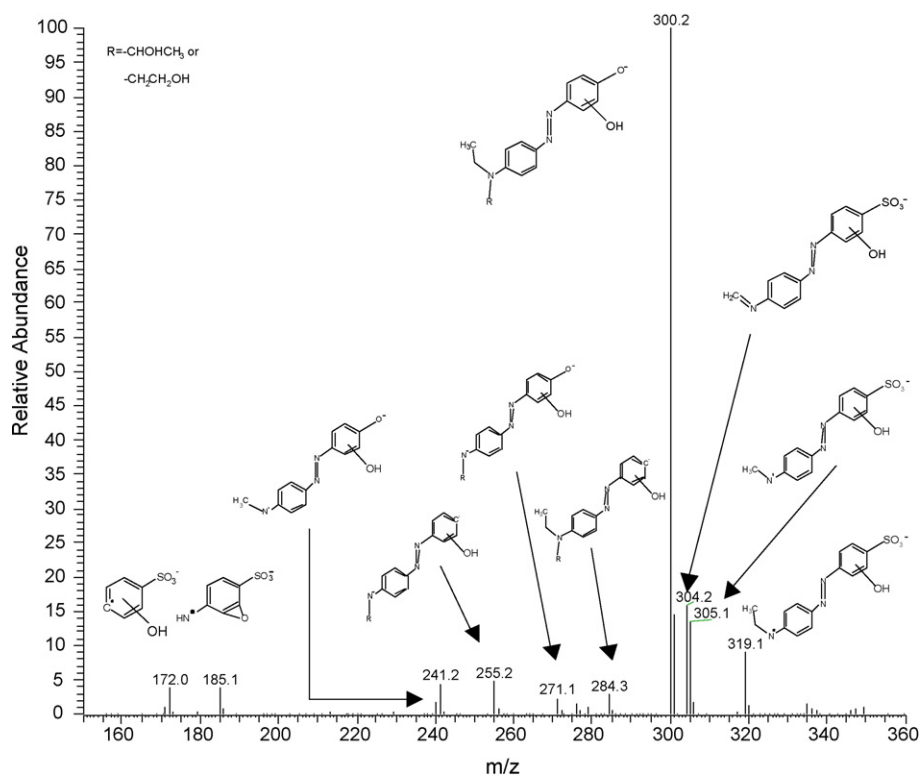
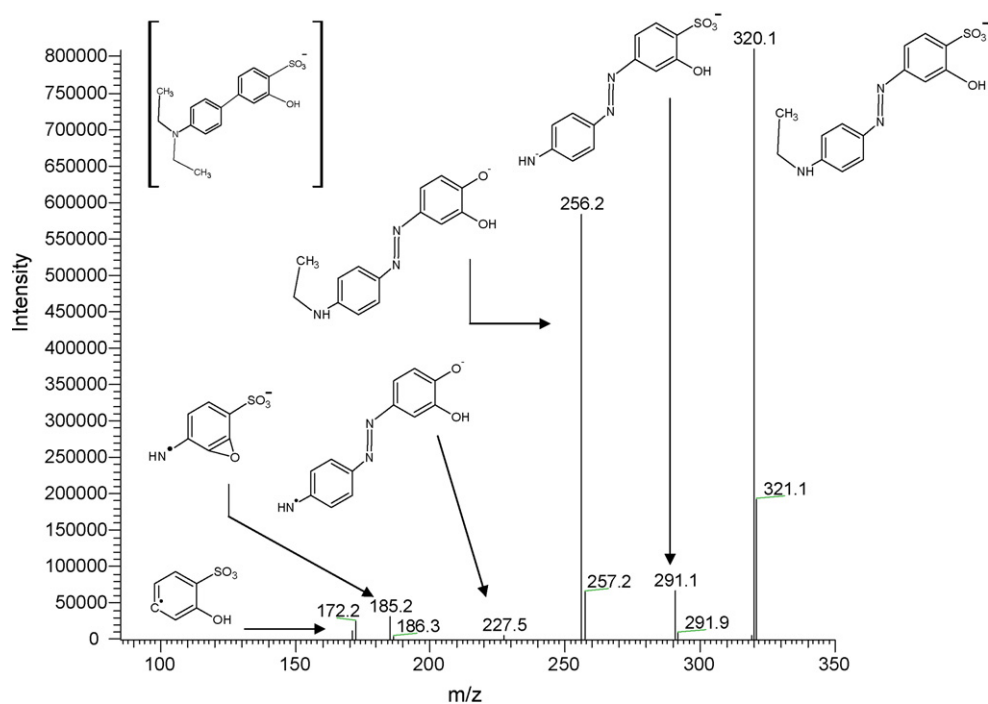**Fig. 6.** MS^2 spectrum and fragmentation of intermediate having *m/z* 364.

Fig. 7. MS^2 spectrum and fragmentation of intermediate having *m/z* 320 and t_R = 15.6 min.

in Table 1). In particular four signals have been found having m/z 320, resulting from both alkyl chain degradation and hydroxylation; two of them ($t_R = 15.1$ and 13.1) exhibit in the corresponding MS^2 spectrum a fragment having m/z 156, accounting for an OH introduction on the N-diethyl-4-aminophenyl ring. Fig. 7 reports the MS^2 spectrum and the fragmentation pathway of the more abundant isomer ($t_R = 15.6$); the absence of the fragment with m/z 156 and the presence of the one having m/z 172 suggest the hydroxylation on the sulfonated ring. In addition, the predominant presence of m/z 256 fragment (loss of SO_2) could be due to an OH attack in *ortho* position to SO_3^- group, stabilizing the structure. No sufficient information can be obtained in order to assess the position of the OH radical attack for the signal at 12.8 min.

For all these three m/z values (276, 304 and 320) in addition to the proposed structures, also the corresponding intermediates coming out from the loss of N_2 instead of C_2H_4 could be hypothesized (see as an example the structure in brackets in Fig. 7), based only on the nominal mass value. Nevertheless this hypothesis has

been rejected since the UV–vis spectrum still shows the absorption band related to the presence of the conjugated azo-group (Fig. 8).

3.2.2. Orange I and Orange II

Table 2 reports the intermediate structures detected in irradiated solutions of OI and OII, respectively; in Figs. 9 and 10 the digital reconstruction at significant m/z values of the chromatogram is shown. In the case of OI all the intermediates elute in a significantly or slightly lower than the parent molecule ($t_R = 15.3$ min), whereas in the case of OII in few cases also intermediates eluting slightly later than the OII itself ($t_R = 16.2$ min) have been detected.

For both OI and OII mono- and dihydroxylated derivatives were found in different isomeric forms, always lower in number than the positions available for an OH introduction; moreover many of these intermediates are present at trace levels and no useful informations were obtained from MS^2 spectra fragmentation in order to attribute the exact structure to each of them.

Table 2
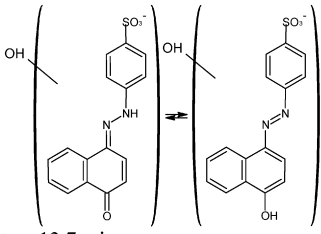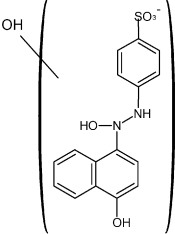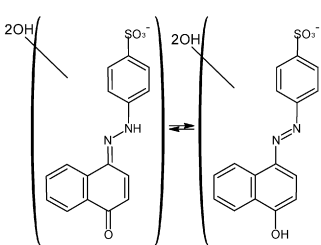Orange I and Orange II degradation: intermediates detected after 15 min irradiation
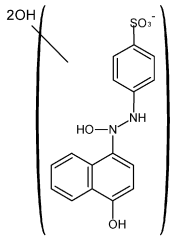
Orange I
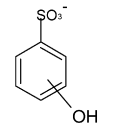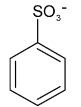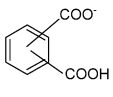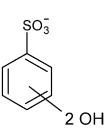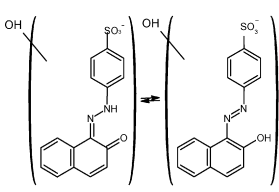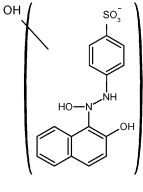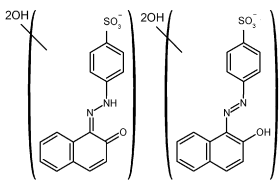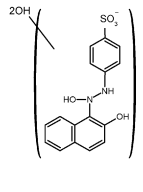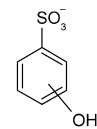
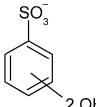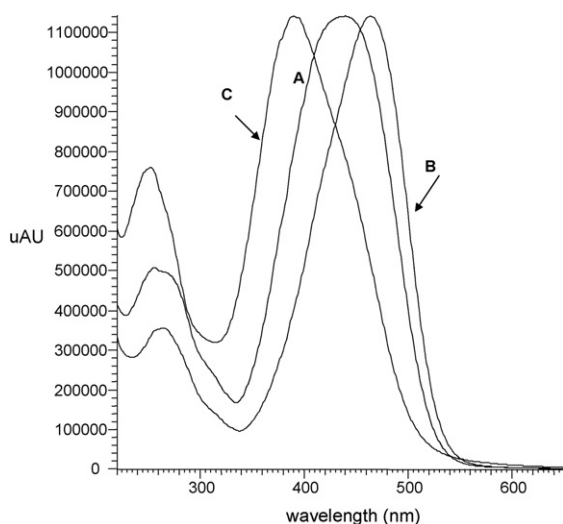| m/z	structure	m/z	structure
343	$t_R = 13.7$ min $t_R = 14.7$ min $t_R = 15.2$ min	361	$t_R = 3.4$ min $t_R = 10.4$ min
359	$t_R = 12.9$ min	377	$t_R = 3.5$ min $t_R = 9.4$ min
173	$t_R = 1.8$ min	157	$t_R = 2.2$ min
165	$t_R = 1.7$ min	189	$t_R = 1.8$ min

Table 2 (*Continued*)

Orange II

m/z	structure	m/z	structure
343	t_R= 14.6 min t_R= 15.3 min t_R= 15.8 min t_R= 16.8 min	361	t_R= 11.4 min t_R= 13.1 min
359	t_R= 16.7 min	377	t_R= 13.0 min
173	t_R= 1.8 min	157	t_R= 2.1 min
165	t_R= 1.5 min	189	t_R= 13.7 min

Fig. 8. UV–vis spectrum of intermediates corresponding to *m/z* 304 (A), *m/z* 320 ((B) *t*_R = 15.6) and *m/z* 276 ((C) *t*_R = 12.3).

Peculiar intermediates, where the conjugation involving the N atoms has been destroyed, and thus not contributing to the solution colour, have also been detected. The formation of such molecules could be related to the fact that OI and OII exist in two tautomeric forms where an H atom is exchanged between O of naphthyl group and the β-hydrogen of the corresponding azo-linkage. In the case of an aqueous solution of OII the two tautomers are in equilibrium, as can be deduced by the UV–vis spectrum showing both the bands corresponding to azo (395 nm) and hydrazone (490 nm) group, whereas the hydrazone form is reported to be prevalent in the presence of TiO$_2$ [27]. No specific indication is given for OI in the presence of TiO$_2$, but the UV–vis spectrum of the corresponding water solution is not showing the azo contribution, thus allowing the hypothesis that also in this case the hydrazo tautomer prevails in the heterogeneous system (Fig. 1). Moreover when the photocatalytic degradation of OI has been attempted only its hydrazone form has been considered [28]. The hydrazone tautomeric form could be responsible of the reactivity of the N atom in the α-position with respect to naphthalene ring.

Products of molecule rupture, such as derivatives of the *p*-hydroxybenzensulfonic acid have been detected for both the dyes at very low concentration even if they are not reported in Table 2.
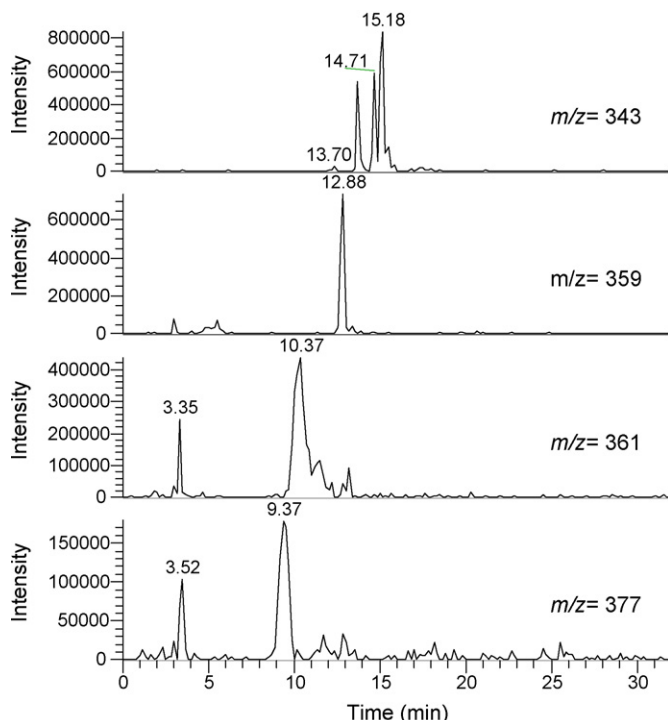
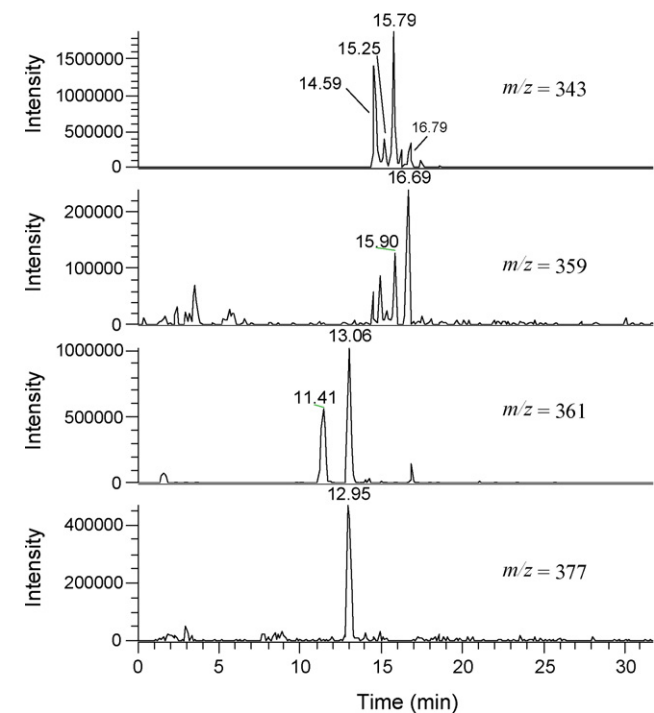**Fig. 9.** LC–MS pattern of the OI sample after 20 min of degradation displayed at different m/z values.

Fig. 10. LC–MS pattern of the OII sample at 15 min of degradation displayed at different m/z values.

4. Conclusion

TiO$_2$ mediated photocatalytic degradation was confirmed as suitable treatment to achieve not only the bleaching rather the complete mineralization of the investigated azo dye aqueous solutions. The chosen analytical approach, based on multistage mass spectrometry along with UV-diode array spectrophotometer, allowed the identification of various sulfonated intermediates, formed at the earlier reaction steps, not reported in previous similar investigations. These compounds appear to be stable enough to accumulate in the system, as revealed by the colour persistence whereas the smaller fragments originated from the molecules breaking showed much faster degradation rates.

Furthermore this study confirmed that LC–MS^n technique demonstrates to be a powerful tool to monitor pollutant compounds and their related degradation compounds in environmental samples, as well at trace level.

References

[1] H. Zollinger, Colour Chemistry: Synthesis, Properties and Applications of Organic Dyes and Pigments, VHS Publishers, New York, 1991.
[2] T. Robinson, G. McMullan, R. Marchant, P. Nigam, Bioresour. Technol. 77 (2001) 247.
[3] E. Weber, N.L. Wolfe, Environ. Toxicol. Chem. 6 (1987) 911.
[4] K.T. Chung, G.E. Fulk, M. Egan, Appl. Environ. Microb. 35 (1978) 558.
[5] N. Willmott, J. Guthrie, G. Nelson, J. Soc. Dyers Colour 114 (1998) 38.
[6] P.C. Vandevivere, R. Bianchi, W. Verstraete, J. Chem. Technol. Biotechnol. 72 (1998) 289.
[7] D. Bahnemann, Sol. Energy 77 (2004) 445.
[8] J.M. Herrmann, Topics Catal. 34 (2005) 49.
[9] I.K. Konstantinou, T.A. Albanis, Appl. Catal. B: Environ. 49 (2004) 1 (and references therein).
[10] Y.X. Chen, S.Y. Yang, K. Wang, J. Photochem. Photobiol. A 172 (2005) 47.
[11] M. Muruganandham, J. Hazard. Mater. 135 (2006) 78.
[12] M. Muruganandham, M. Swaminathan, Dyes Pigments 681 (2006) 33.
[13] C. Hu, X.X. Hu, L.S. Wang, Environ. Sci. Technol. 40 (2006) 7903.
[14] T. Velegraki, I. Poulios, M. Charalabaki, Appl. Catal. B 62 (2006) 159.
[15] M. Stylidi, D.I. Kondarides, X.E. Verykios, Appl. Catal. B. 47 (2004) 189.
[16] I. Dalmazio, A.P.F.M. de Urzedo, T.M.A. Alves, R.R. Catharino, M.N. Eberlin, C.C. Nascentes, R. Augusti, J. Mass Spectrom. 42 (2007) 1273.
[17] C. Baiocchi, M.C. Brussino, E. Pramauro, A. Bianco Prevot, L. Palmisano, G. Marcì, Int. J. Mass Spectrom. 214 (2002) 247.
[18] F. Kiriakidou, D.I. Kondarides, X.E. Verykios, Catal. Today 54 (1999) 119 (and references therein).
[19] C. Bauer, P. Jacques, A. Kalt, J. Photochem. Photobiol. A 140 (2001) 87.
[20] J. Bandara, J.A. Mielczarski, J. Kiwi, Langmuir 15 (1999) 7670.
[21] Y. Chen, S. Yang, K. Wang, L. Lou, J. Photochem. Photobiol. A 172 (2005) 47.
[22] L. Lucarelli, V. Nadtochenko, J. Kiwi, Langmuir 16 (2000) 1102.
[23] K. Vinodgopal, D. Wynkoop, P. Kamat, Environ. Sci. Technol. 30 (1996) 1660.
[24] S. Yang, L. Lou, K. Wang, Y. Chen, Appl. Catal. A 301 (2006) 152.
[25] E. Puzenat, H. Lachheb, M. Karkmaz, A. Houas, C. Guillard, J.M. Herrmann, Int. J. Photoenergy 5 (2003) 51.
[26] G. Palmisano, M. Addamo, V. Augugliaro, T. Caronna, A. Di Paola, E. Garcia Lopez, G. Marcì, L. Palmisano, M. Schiavello, Catal. Today 122 (2007) 118.
[27] C. Bauer, P. Jacques, A. Kalt, Chem. Phys. Lett. 307 (1999) 397.
[28] C. Galindo, P. Jacques, A. Kalt, Chemosphere 45 (2001) 997.